Expandable Graphite Systems for Halogen-Free Flame-Retarding of Polyolefins. II. Structures of Intumescent Char and Flame-Retardant Mechanism

RONGCAI XIE, BAOJUN QU

State Key Laboratory of Fire Science and Department of Polymer Science and Engineering, University of Science and Technology of China, 230026 Hefei, Anhui, People Republic of China

Received 21 January 2000; accepted 24 July 2000

ABSTRACT: The structures of the intumescent charred layers formed from polyolefin (PO) blends with expandable graphite (EG) and/or the other free-halogen flame retardant (HFFR) and their flame-retardant mechanism were studied by Fourier transform infrared (FTIR) spectroscopy, X-ray photoelectron spectroscopy (XPS), laser Raman spectroscopy (LRS), scanning electron microscopy (SEM), differential thermal analysis (DTA), and thermal conductivity (TC) measurements. The FTIR, XPS, and LRS data showed that the carbonaceous structures of intumescent charred layers consist of EG and various numbers of condensed benzene rings and/or phosphocarbonaceous complexes attached by the P—O—C and P—N bonds or quaternary nitrogen or dehydrated zinc borate (ZB). These results and the morphologic structures observed by SEM have demonstrated that the compact structures of charred layers slow down heat and mass transfer between the gas and condensed phase and prevent the underlying polymeric substrate from further attack by heat flux in a flame. The DTA data provide the positive evidence for the flame-retardant mechanism of the PO/EG/HFFR systems, which works by increasing the oxidation temperature and decreasing thermal oxidation heat. At the same time, the TC data reveal the flame-retardant essence of the charred layers as good heat-insulated materials whose TC value is only about 1/10 of the corresponding blend.
 J Appl Polym Sci 80: 1190–1197, 2001

Key words: expandable graphite; intumescent char structure; polyolefin; thermal conductivity; halogen-free flame retardant

INTRODUCTION

It has been known for many years that an intumescent process can provide fire protection for flammable materials.[1] The first article in this series[2] reported on the study of expandable graphite (EG) as an intumescent flame-retardant (FR) additive of polyolefins (PO) and its synergistic effect with other halogen-free flame-retardant (HFFR) additives. According to our studies, EG is a very efficient intumescent FR additive that performs both as a carbonization compound and as a blowing agent. EG systems combined with other FRs have excellent fireproofing properties in that the blends burn slowly and smoothly and are accompanied by a large decrease in the HRR and EHC values. The data from the TGA and cone calorimeter tests have shown that the synergistic effect of EG with other HFFR additives significantly promotes the formation of carbonaceous char in the PO/EG/FR blend materials. The proposed mechanism for this is the foamed cellular

Correspondence to: B. Qu (qubj@ustc.edu.cn).
Journal of Applied Polymer Science, Vol. 80, 1190–1197 (2001)

charred layers formed on heating acting as a physical barrier on the surface of blends, a process that slows down heat and mass transfer between the gas and condensed phase and protects the underlying materials from heat flux or a flame. However, this mechanism needs to be experimentally proven. As far as we are aware, the structure of charred layers and the flame-retardant mechanism of EG systems have not been reported about in the literature.

This article mainly reports on our investigation—using Fourier transform infrared (FTIR) spectroscopy, X-ray photoelectron spectroscopy (XPS), laser Raman spectroscopy (LRS), scanning electron microscopy (SEM), differential thermal analysis (DTA), and thermal conductivity (TC) measurement—of the chemical composition and structure of the intumescent charred layers formed in these systems. The article then also discusses the flame-retardant mechanism of EG with other HFFR additives in the polyolefin blend.

EXPERIMENTAL

Materials

The two kinds of polyolefins used in the present work were linear low-density polyethylene (LLDPE, DFDC-7050) from the Zhongyuan Oil Company and ethylene vinyl acetate copolymer (EVA, containing 19% vinyl acetate) from the Yanshan Company. Expandable graphite with a high expansion coefficient of 180 (HEG) and a low expansion coefficient of 40 (LEG) was supplied by Baoding Lianxing Carbide Company, Ltd. The particle size of HEG was 0.2 mm, with a pH value of 8.5; the particle size of LEG was 100 mesh with a pH value of 7.2. The following HFFR additives were used in this work: ammonium polyphosphate (APP) from Anhui Institute of Chemical Engineering, zinc borate $2ZnO3B_2O_33.5H_2O$ (ZB) from Gaizhou Inorganic Chemicals Company, and the phosphorus–nitrogen compound NP28 from Weizheng Fine Chemicals Company. The NP28 containing 15.6% P and 27.5% N had a particle size of 400 mesh. A microcapsulated red phosphorus (RP) was made in our laboratory. All the above chemicals except RP are commercial products made in China and used as received.

Sample Preparation

Blend samples, consisting of 100-g batches of PO with the desired amounts of EG and HFFR additives, were mixed for 15 min at 115–130°C using a rubber mill. After mixing, the samples were hot-pressed under 10 MPa for 10 min at 130–150°C into sheets or pellets of suitable thickness. Sheet size and thickness were dependent on the testing methods used in the present study.

Table I Char Samples and Corresponding Blends Used for FTIR and XPS

Char Sample No.	Composition of Blend	Burning Time, *s*
1	A[a] + 5% RP + 15% APP	4
2	A + 5% RP + 15% APP	10
3	A + 5% RP + 15% NP28	10
4	A + 20% ZB	10
5	A	10
6	B[b] + 5% RP + 15% NP28	10

[a] A = 70% LLDPE + 10% LEG.
[b] B = 70% EVA + 10% LEG.

The char samples (without special illustration) were obtained from burning the corresponding blends vertically in a flame for 10 s. Only one incompletely burned char sample, obtained from burning for 4 s, was used for a comparison of FTIR spectra. The chars were pressed into pellets at 10 MPa for the LRS measurements or kept in their original state for the other use. The compositions and preparation conditions of the char samples and corresponding blends used for the FTIR and XPS measurements are listed in Table I.

Analysis of Sample

FTIR Spectra

The FTIR spectra of each char sample in a KBr pellet were recorded with a Nicolet MAGNA-IR 750 spectrometer.

Laser Raman Spectroscopy

The laser Raman spectroscopy (LRS) measurements were carried out at room temperature with a SPEX-1403 laser Raman spectrometer, with excitation provided in backscattering geometry by a 514.5-nm argon laser line.

XPS Spectra

The XPS spectra were recorded with a VG ESCALAB MK II spectrometer, using Al kα excita-

tion radiation (hv = 1253.6 eV), and were calibrated by assuming the carbonaceous carbon to be 284.6 eV.

SEM Analysis

The SEM micrographs of surfaces and cross sections of the charred layers were analyzed by a X650 scanning electron microscopy (Hitachi X560 scanning electron microanalyzer). The specimens were previously coated with conductive gold layer.

DTA Measurements

DTA data were obtained from a simultaneous TG-DTA instrument(STA 409C thermogravimetric analyzer) at a heating rate of 10°C/min in air. The flow rate of carrier gas was 60 mL/min.

Thermal Conductivity Measurements

To do the thermal conductivity (TC) measurements, a metal line of standard copper–nickel (Omega Group Company) for measuring temperature was located in the middle of two identical blends (90 mm × 30 mm × 30 mm). Two lines of copper joined by fusion to the above-mentioned wire were connected with a thermal conductometer. One probe of the thermal conductometer was placed in a cylinder (40 mm in height, 10 mm in diameter) in which the char was piled up naturally. In this way the thermal conductivity of the blends and corresponding chars was obtained. The thermal conductometer was previously calibrated with glycerin.

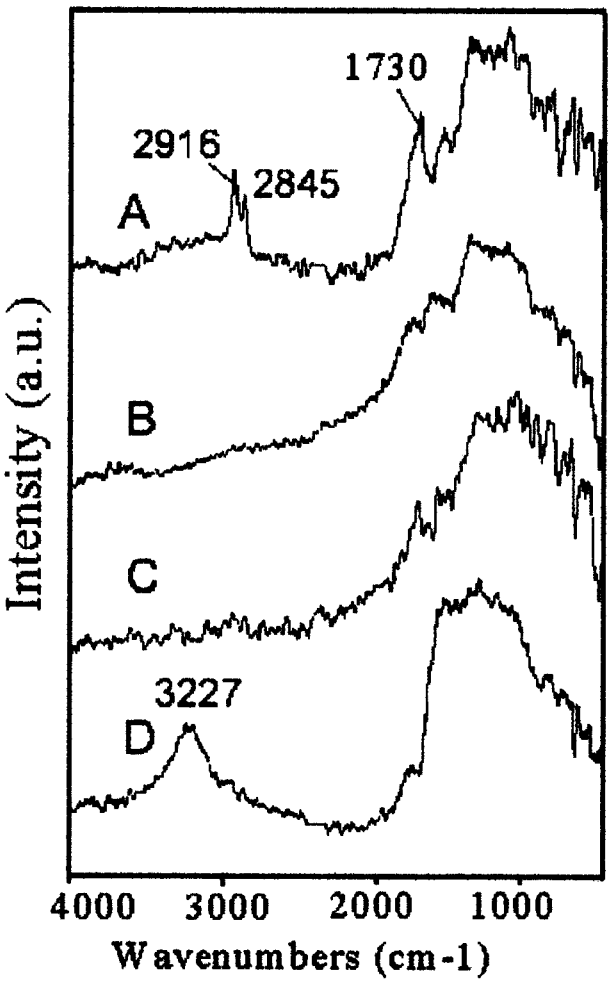

Figure 1 FTIR subtraction spectra obtained from the LLDPE/10% EG/HFFR char samples minus the background spectrum of the LLDPE/10% EG char sample. Spectra A, B, C, and D were obtained, respectively, from the spectra of samples 1, 2, 3, and 4 minus the background spectrum of sample 5. The symbols for the samples are listed in Table I.

RESULTS AND DISCUSSION

FTIR Analysis of Charred Layers Obtained from LLDPE Blends

Figure 1 presents the FTIR subtraction spectra obtained from samples 1–4 minus the background spectrum of sample 5 (Table I). In order to characterize the structures and compositions of the intumescent charred layers formed from the blends with different FR additives, we used the technique of an FTIR subtraction spectrum in the present study to reduce the effect of the EG itself. Curves A, B, C, and D in Figure 1 represent, respectively, the subtraction spectra obtained from samples 1, 2, 3, and 4 minus the background spectrum of sample 5. The two additional absorption peaks, at 2916 cm^{-1} and 2845 cm^{-1}, in Figure 1(a) can be ascribed to symmetric vibration of the aliphatic groups $(—CH_2—)_n—$, as had been reported in the literature[3] for the incompletely burned hydrogen–carbon compound. The absorption around 1730 cm^{-1} is a result of the carbonyl groups. The broad signals at 1150–1300 cm^{-1} of Figure 1(a–c) have been assigned to the P—O—C bonds in the phosphocarbonaceous complexes or the P═O bonds in the phosphate complexes, as reported in the literature.[4] The small absorption peaks between 900 cm^{-1} and 1150 cm^{-1} in Figure 1(a–c) have been assigned to the symmetric vibration modes of PO_2, PO_3, and the asymmetric or symmetric vibration modes of a

P—O bond in a P—O—P chain in the literature.[5] The P—O bonds were from the oxidation of RP and the decomposition of the APP and NP28 compounds. The peak at 3227 cm^{-1} in Figure 1(d) is characteristic of dehydrated zinc borate,[6] which means that $2ZnO3B_2O_33.5H_2O$ was dehydrated into $ZnO3B_2O_3$ and mixed with a carbonaceous structure during combustion.

By comparing Figure 1(a) with Figure 1(b), it can be seen that the incomplete combustion sample (sample 1) has a higher intensity at 1730 cm^{-1}, meaning there are more carbonyl groups in the char of sample 1 that have not been decomposed into the gaseous phase. Several small peaks at 900–1150 cm^{-1} in Figure 1(b) disappear, and the intensity of the broad peaks at 1150–1300 cm^{-1} increases, indicating the P—O—P or PO_2 or PO_3 bonds have been mainly transferred into the P—O—C or P═O bonds in the completely burning sample of Figure 1(b). Additional detailed information about the dynamic thermo-oxidative degradation processes of the PO/EG/HFFR blends in the condensed phase will be presented in a later article in this series.[7]

XPS Analysis of Charred Layers Obtained from PO/EG/HFFR Blend Systems

XPS provided detailed information about element composition and content of the blend and charred layers, which complement the results from infrared spectroscopy. Figure 2 shows the C_{1s}, P_{2p}, and N_{1s} XPS spectra of the char obtained from the LLDPE/EG/HFFR blends (sample 3 in Table I) after vertically burning for 10 min. It can be seen that the C_{1s} main peak of the char sample appears at 285 eV. But there exist two weak peaks, marked by broken lines in the C_{1s} spectrum of Figure 2. One is at 289.2 eV, which has been assigned to the carboxyl group in the literature.[8] The other, a shoulder peak, is at 286.2 eV, which might be a result of the formation of P—O—C groups or other C—O compounds.

The P_{2p} XPS spectrum in Figure 2 presents the characteristic peak of intumescent char obtained from sample 3. Usually the binding energy of P_{2p} of inorganic phosphorus is 130 eV, whereas the P_{2p} peak of char sample appears at 134.5 eV. The great increase of P_{2p} binding energy indicates the formation of oxidation products of the phosphate species. It has been reported in the literature[9] that the binding energy of the P—O—C and/or PO_3^- in phosphate species and/or P_2O_5 was located at about 134–135 eV. These results provide evidence that inorganic and organic phosphorus in LLDPE/EG/HFFR blends has been converted into phosphocarbonaceous complexes in the char

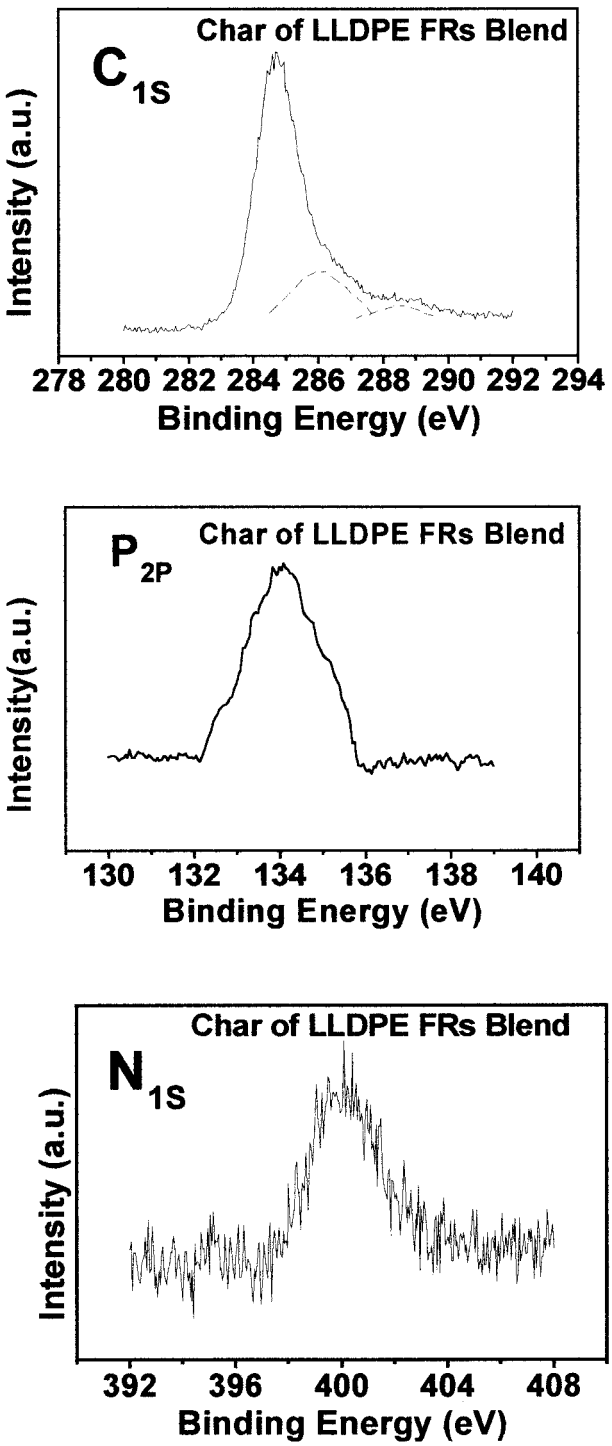

Figure 2 C_{1s}, P_{2p}, and N_{1s} XPS spectra of the char samples obtained from LLDPE/EG/HFFR blends (sample 3 in Table I).

after burning, which is in good agreement with the results of the IR spectrum previously mentioned.

The N_{1s} main peak of the same char sample in Figure 2 is at 400 eV, whereas the shoulder peak appears at 401 eV, which could be a result of the formation of quaternary nitrogen and to some formation of oxidized nitrogen compounds, as reported in the literature.[10]

Figure 3 shows the C_{1s}, P_{2p}, and N_{1s} XPS spectra of the EVA/EG/HFFR blend (sample 6 in Table I) and the corresponding char. It can be seen that the C_{1s} XPS main peaks of the blend and char samples also appear at 285 eV. At the same time the very weak peak at 289.3 eV from the blend sample has been assigned to the carboxyl group, and the shoulder peak at 286.2 eV has been assigned to the P—O—C groups or other C—O bonds, as described in the C_{1s} peak of Figure 2.

Figure 3 only shows the P_{2p} spectrum of the intumescent char obtained from sample 6 of the EVA/EG/HFFR blend. The P_{2p} peak of the blend was not observed, probably because the microcapsulation of the RP and NP28 additives in the blends, in which the average coating thickness of MRP was above the detectable range of the XPS method. The binding energy of P_{2p} also shifts upward to 134.5 eV, similar to the P_{2p} peak of the char from the LLDPE/EG/HFFR system. The increase of P_{2p} binding energy is a result of the formation of oxidation products of the phosphate species, such as P—O—C, PO_3^-, and P_2O_5. The N_{1s} spectra of the EVA blend and char from sample 6 are also shown in Figure 3. The N_{1s} peak of the blend appears at 400 eV, but the N_{1s} peak of the char becomes wider and has shifted 1 eV upward to 401 eV, which has been assigned to quaternary nitrogen and to some formation of oxidized nitrogen compounds.[10]

The above results provide evidence that the products that result in the char after the burning of the EVA/EG/HFFR blends are similar to those of the LLDPE blends with the same additives.

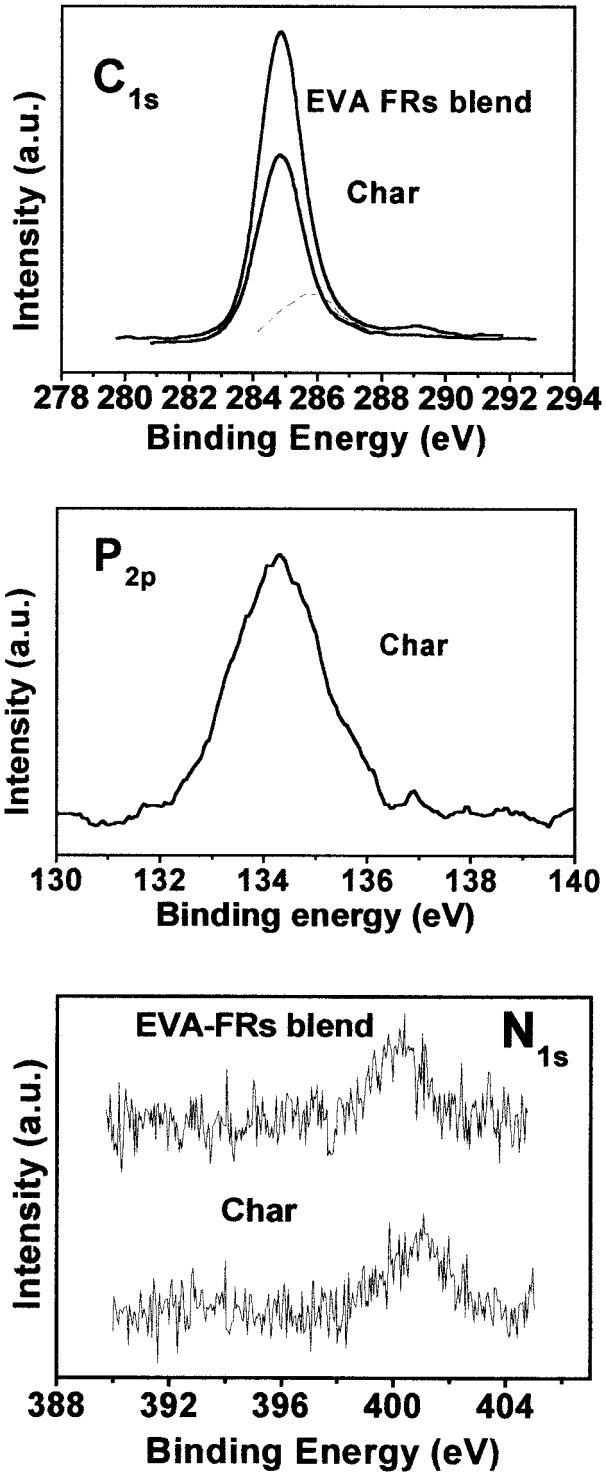

Figure 3 C_{1s}, P_{2p}, and N_{1s} XPS spectra of EVA/EG/HFFR blends (sample 6 in Table I) and corresponding char samples.

Structure Characterization of Intumescent Charred Layers

Because an IR spectrum and XPS cannot identify types of carbonaceous structures, we were prompted to examine the structural characteristics of the "carbon" on the intumescent materials. In this work laser Raman spectroscopy was used to characterize the different types of carbonaceous structures formed in the intumescent char. Figure 4 presents laser Raman spectra of five samples. It can be seen that four of the five sam-

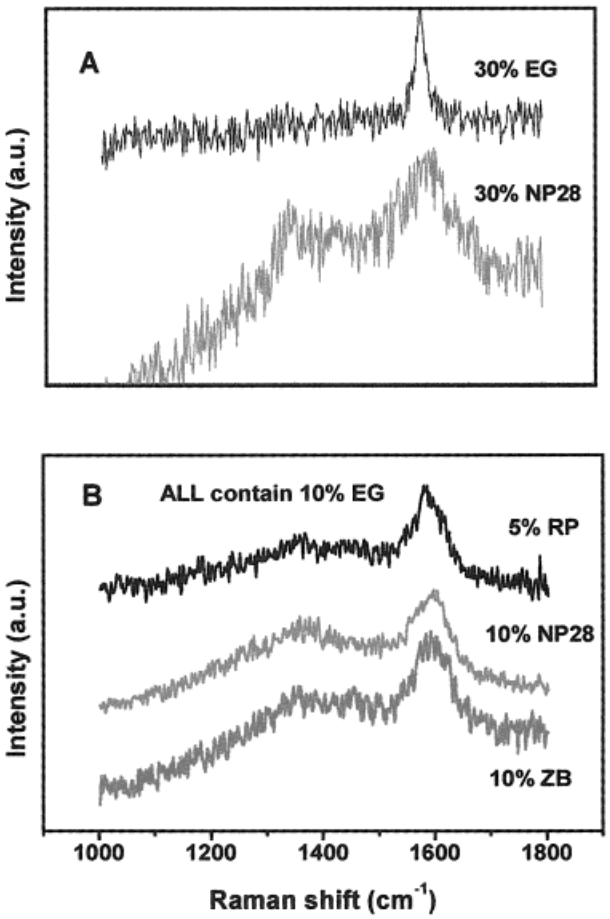

Figure 4 Laser Raman spectra of the intumescent char samples obtained from LLDPE blends with different HFFR additives: (a) LLDPE blends with 30% EG or 30% NP28 only; (b) 10% EG–based LLDPE blends with different HFFR additives of 5% RP, 10% NP28, and 10% ZB. [Color figure can be viewed in the online issue, which is available at www.interscience.wiley.com.]

ples, except for the LLDPE/30% EG sample, have a common feature of two distinct broad peaks centered approximately at 1575 cm^{-1} (G line) and 1350 cm^{-1} (D line). However, the positions, widths, and relative intensities of these two peaks are quite different in the various samples. In Figure 4(a), the char sample containing only 30% EG shows a sharp peak at 1575 cm^{-1}. It has been reported[11] that the 1575 cm^{-1} peak has been assigned to the Raman active $2E_{2g}$ modes of C—C vibrations in graphite. In contrast with the 30% EG sample, the char sample with 30% NP28 shows a stronger intensity and broader width peaks at 1575 cm^{-1} (G line) and 1350 cm^{-1} (D line), indicating the carbonaceous structures of intumescent char are highly disordered. The Raman D line at 1350 cm^{-1} represents the disorder structure, which may be a result of the alternating ring stretch vibration of benzene or of aromatic clusters, as has been reported in the literature.[12–13]

In Figure 4(b) the intumescent char samples formed from the different contents of RP, NP28, and ZB in the LLDPE/10% EG blends also show a broader G line (about 1575 cm^{-1}) and a new broad D line (1350 cm^{-1}), as compared with that of the char peak from the LLDPE/30% EG blends. The broadening G line and the new D line indicate more disordered structures of the intumescent char in these systems. This is because these systems contain various numbers of condensed benzene rings with different sizes and different environments incorporated into the expanded graphite. The upward shift of the Raman peak (G line) to about 1588 cm^{-1} might be because of sp^2 stretching vibration of aromatic rings in the benzene or fused-benzene clusters.[12] Meanwhile, C═C sp^2 stretch vibrations of olefinic or conjugated carbon chains exhibit a Raman peak at about 1620 cm^{-1}. The downward shift may be because of the high hydrogen content, the superposition of the semicircle stretching at 1486 cm^{-1} vibration in benzene or benzene clusters, and the local environment of the benzene cluster as well as cluster size and stress. The ZB sample in Figure 4(b) shows broader G (about 1575 cm^{-1}) and D (1350 cm^{-1}) line than those of the RP or NP28 system. This might indicate that the ZB additive can also promote the formation of condensed char layers.

Morphologic Structures of Intumescent Chars from Different LLDPE/EG/FR Systems

The SEM photos of chars from the surfaces of various fire samples are presented in Figure 5. Figure 5(a) shows that the chars of LLDPE/30% HEG blend nearest to the flame expand into a wor-like material, as reported in the literature,[14] whereas Figure 5(f) shows the swell chars next to the flame, which are being expanded as a leaflike overlapped morphological structure. From these pictures it can be imagined that expanded graphite with different expansion coefficients because of different environmental temperatures intercross and overlap between flame and blends. Figure 5(b–e) shows the SEM photos of chars from the different LLDPE blends with the ZB, NP28, APP, and RP at the same level of additive, respectively. Figure 4(b) seems very compact, but this

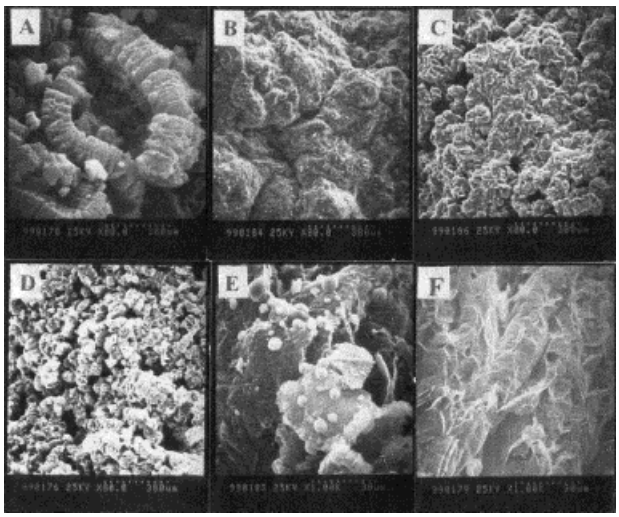

Figure 5 SEM micrography of the intumescent char samples obtained from LLDPE blends with EG or EG and HFFR additives: (a) 30% HEG × 53; (b) 10% LEG + 15% ZB × 53; (c) 10% LEG + 15% NP28 × 53; (d) 10% LEG + 15% APP × 53; (e) 18% LEG + 7% RP × 667; (f) 30% HEG × 667 (original magnification).

formulation could not pass the V–0 ratings of the UL-94 test. Figure 4(e) shows some small balls stuck to the large EG flakes. Similarly, Figure 5(c,d) shows small "carbon" balls stuck to the surface of EG. However, the char from the LLDPE/LEG/NP28 sample seems more compact than that from the LLDPE/LEG/APP sample. This provides additional evidence that NP28 has a better synergistic effect with EG than does APP.

DTA Analysis of Thermal Oxidation Stability

The DTA data of the thermo-oxidative degradation temperatures and the intensities of oxidation peaks for the LLDPE/EG and LLDPE/EG/FR blends are listed in Table II. The oxidative degradation temperatures of LLDPE/EG or LLDPE/EG/FR samples increase from 393°C of the pure LLDPE to 419–465°C, whereas the intensities of oxidation peaks decrease from 812 J/g of the pure LLDPE to 130–593J/g, depending on the different compositions of FR additives. This is because the charred layers containing expanded graphite or incorporated with the condensed benzene and benzene clusters or phosphocarbonaceous complexes can protect the underlying LLDPE materials from the heat oxidation process and lead to the increase of oxidation temperature and a remarkably significant decrease of oxidation peak intensity. Apparently, the LLDPE/10% LEG blend with 5% RP and 15% NP 28 is the most efficient among these sample systems because it has the highest oxidation temperature (465°C) and the lowest oxidation intensity (220 J/g). These results provide positive evidence that the flame-retardant mechanism of EG systems in the polyolefin materials works by increasing oxidation temperature and decreasing oxidation heat.

Thermal Conductivity of Intumescent Chars

Table III lists the data for thermal conductivity (TC) determined from the LLDPE/EG or LLDPE/EG/FR blend samples. It can be seen from Table III that the TC values of blends increase from 0.32 W/mK of pure LLDPE to 0.41–0.58 W/mK. The TC values of the intumescent chars are only about 1/10 of the corresponding blend samples. In fact, intumescent charred layers with very small TC values (0.048–0.099 W/mK) have become

Table II Comparison of Oxidization Peak Temperatures and Oxidization Intensities Measured by DTA

FR Content in LLDPE (%)	Oxidization Peak Temperature (°C)	Oxidization Peak Intensity (J/g)
0%	393	812
10% HEG	412	564
30% HEG	430	310
10% LEG	405	590
30% LEG	438	322
10% LEG + 10% ZB	450	593
10% LEG + 10% APP	421	553
10% LEG + 10% NP28	448	408
10% LEG + 5% RP + 15% ZB	460	253
10% LEG + 5% RP + 15% NP28	465	220

Table III TC Data of LLDPE Blend and Char Samples

FR Content in LLDPE (%)	Thermal Conductivity (W/m K)	
	Resin or Blend	Char
Pure LLDPE	0.32	—
30% HEG	0.56	0.048
30% LEG	0.58	0.063
10% LEG + 20% ZB	0.47	0.063
10% LEG + 15% NP28 + 5% RP	0.41	0.099

quite good heat-insulated materials. These TC data reveal the flame-retardant essence that the intumescent charred layers formed by heating or combustion of materials are quite good heat-insulated materials that protect the underlying polymeric materials from further thermal oxidation degradation.

CONCLUSIONS

The carbonaceous structures of the intumescent charred layers formed in the PO/EG/HFFR systems and their flame-retardant mechanism observed by FTIR, XPS, LRS, SEM, DTA, and TC measurements in the present work can be summarized as follows:

1. The carbonaceous structures of intumescent charred layers formed from the polyolefin blends with EG and/or other HFFR additives consist of expanded graphite and various numbers of condensed benzene rings or benzene clusters and/or phosphocarbonaceous complexes attached by P—O—C and P—N bonds or quaternary nitrogen. The char structure of the blend system with EG and ZB additive is mainly composed of expanded graphite and dehydrated ZB.
2. Based on our structure studies, it was determined that the flame-retardant mechanism is the compact charred layer acting as a physical barrier, which slows down heat and mass transfer between the gas and condensed phases and prevent the underlying polymeric substrate from further attack from flame or heating.
3. The DTA data provide positive evidence that the flame-retardant mechanism of EG/FR systems in the polyolefin materials works by increasing oxidation temperature and decreasing oxidation heat.
4. The TC data revealed that the flame-retardant essence of the intumescent charred layers are quite good as heat-insulating materials, which protect the underlying polymeric materials from further thermal oxidation degradation.

The authors gratefully acknowledge the support of the Knowledge-Creating Engineering Fund of the Chinese Academy of Sciences, which provided a grant for this project.

REFERENCE

1. Camino, G.; Costa, L.; Trossarelli, L., Polym Deg Stab 1984, 7, 25.
2. Xie, R. C.; Qu, B. J. J Appl Polym Sci, to appear.
3. Craver, C. D. The Coblenz Society Deskbook of Infrared Spectra; Kirwood, 1980.
4. MacKee, D. W.; Spiro, C. L.; Lamby, E. J. Carbon 1984, 22 285.
5. Bourbigot, S.; Bras, M. L.; Delobel, R.; Tremillon, J. M. J Chem Soc Faraday Trans 1996, 92, 3435.
6. Inorganic IR Grating Spectra, Sadtler Research Laboratories Inc., Philadelphia, PA, 1972.
7. Xie, R. C.; Qu, B. J.; Hu, K. L. J Appl Polym Sci, submitted.
8. Bourbigot, S.; Bras, M. L.; Delobel, R.; Gengembre, L. Appl Surf Sci 1997, 120, 15.
9. Jansen, R. J. J.; Bekkum, H. V. Carbon 1995, 33, 1021.
10. Beamson, G.; Briggs, D. High Resolution XPS of Organic polymers; Wiley: Chichester, 1992.
11. Tuinstra, F.; Koenig, J. L. J Chem Phys 1970, 53, 1126.
12. Schwan, J.; Ulrich, S.; Batori, V.; Ehrhardt, H.; Silva, S. R. J Appl Phys 1996, 80, 440.
13. Tamor, M. A.; Vassell, W. C. J Appl Phys 1994, 76, 3823.
14. Piotr, P.; Ryszard, O.; Daniel, K. Proceedings of European Flame Retardant Conference 2000; p 105.